

Slumping at the late Miocene shelf-edge offshore West Sabah: a view of a turbidite basin margin

BRUCE LEVELL and AWANG KASUMAJAYA
Sabah Shell Petroleum Co. Ltd., Lutong, Sarawak

Abstract: A coalescing series of elongate spoon or scoop-shaped unconformities can be mapped along approximately 150 km of the 250 km long late Miocene shelf-edge offshore West Sabah. In many cases the unconformities both truncate and are overlain by marine sediments and they are interpreted as being due to retrogressive submarine slumping. Subsequent modification by erosional turbidity currents may have occurred, but most unconformities retain a smooth slump scar morphology.

Two areas with well developed slump scars are described:

- (1) *Samarang Area:* Slump scars have been cut into a 500 m thick sequence of seismically-foresetted slope clays and overlying shallow-water topsets on the upthrown side of a major normal fault. Earthquake activity and slope instability along a submarine fault scarp are thought to have been responsible for the slumping. Failure occurred in either one single event or a series of events closely spaced in time.
- (2) *St. Joseph Area:* Slump scars are cut into slope and shallow water sediments deposited on a flank which was rotating down towards the basin, resulting in slope oversteepening. Slumping occurred repeatedly during the deposition of a 1.5–2 km thick section over a relatively long time period. The proximity of the slump scars to the palaeo-coastline resulted in extensive deposition of sandy turbidites further offshore.

In both areas the dimensions of the slump scars are remarkably similar. Typically 1–5 cubic kilometres of sediments were re-deposited down-slope during slumping and subsequent erosion.

Four exploration wells have penetrated the slump scar unconformities and their fills. With one exception, the fill consists of a monotonous deep water claystone succession. On seismic sections the fill is normally poorly reflective and shows weak seismic foresetting indicative of slope progradation.

The slump scars have a two-fold significance for hydrocarbon exploration:

Firstly the relief created between neighbouring slump scars, overlain by slope clays provides potential for stratigraphic trapping.

Secondly the unconformities allow identification of the stratigraphic units which have been redeposited basinward. Hence the sand-proneness of a turbidite basin can be indirectly assessed. Offshore West Sabah there is a clear relationship between the destructive slope and a major sand-bearing turbidite basin in the northern part of the area.

The widespread occurrence of slump scars in the late Miocene of offshore West Sabah is attributed to active linear basement fault zones which acted as basin margins, and rapid progradation of a thick clastic sequence, possibly aided by an early late Miocene (global) fall in sea level.

INTRODUCTION

The West Sabah continental margin (Fig. 1) represents a 250 km long segment of a

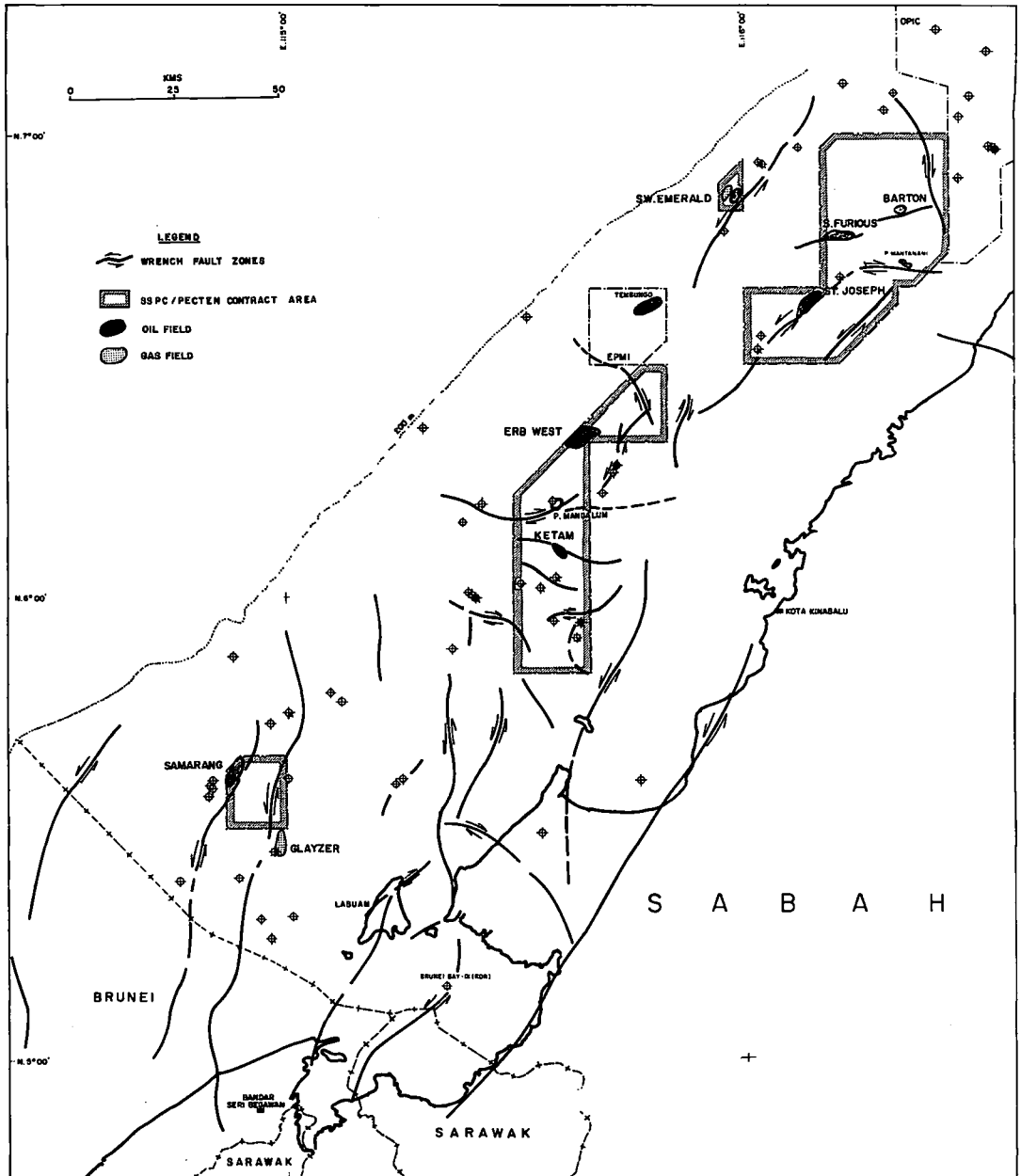


Fig. 1. West Sabah offshore: major wrench fault zones in cover. Sedimentation and structuration of the West Sabah continental margin in the Neogene are thought to have been controlled by basement wrench faults (Bol and van Hoorn, 1980). Several of the N-S to NE-SW trending fault systems have vertical throws of 1000' or more and generally downthrow to the west. These faults have acted as tectonic shelf edges during progradation of a clastic wedge from the southeast. (N.B. indicated movement directions are inferences only).

destructive plate margin along the 1000 km long, presently inactive, Palawan subduction zone (Hamilton 1979, Holloway 1981).

The West Sabah continental shelf is approximately 100 km wide to the 200 m isobath and is underlain by up to 12 km of predominantly Neogene clastic sediments. These are thought to overlie Palaeogene to Late Cretaceous complexes consisting of deep water clastic sediments, cherts and ophiolitic melanges (Hamilton, 1979).

The structural style of the West Sabah continental shelf (Fig. 1) is controlled by two intersecting sets of fault zones: a more extensive N-S to NE-SW striking set and a subordinate E-W striking set (Bol and van Hoorn, 1980).

The N-S to NE-SW striking set is roughly parallel to palaeocoastlines and successively seaward fault zones have acted as progressively younger shelf edges during outbuilding of the Neogene clastic wedge towards the NW. The fault zones are typically between 20–70 km long, straight, and have a complex movement history involving substantial dip-slip (up to 1.5 kms). In many cases movement along an original normal (down-to-basin) fault has been reversed leading to the present day expression of the fault system as a reverse fault zone with a steep, narrow “ridge”-like anticlinal culmination. Based on the fault patterns in cross-section and some poorly established lateral offsets it is surmised that many of the N-S to NE-SW trending fault zones have a strike-slip component. A sinistral displacement sense would be consistent with both some possibly laterally-offset structural features and regional plate tectonics (taking into account the relative orientations of the spreading centre in the South China Sea and the Palawan trough, Holloway, 1981).

The Neogene succession of the West Sabah offshore (Fig. 2) is variable along strike due to tectonic compartmentation into four sub-basins: the Southern, Central and Northern parts of the inner offshore, which are middle to late Miocene sub-basins, and the essentially Pliocene sub-basin of the outer offshore. The Miocene depositional history and succession can however be simplified as follows (Fig. 2):

1. Middle Miocene regional relative sea level fall resulting in unconformable deposition of terrestrial deposits on a deformed early Miocene deep-water sequence in the inner part of the shelf and a conformable progradational sequence to the northwest.
2. A late Mid-Miocene to early late Miocene period of rapid relative sea level rise which resulted in transgression over the whole area and widespread deposition of marine shales with local carbonates.
3. A late Miocene period of slower relative sea level rise (or an increase in clastic input) which resulted in rapid progradation of the shelf edge to a line roughly half way between the present coast and the 200 m isobath.
4. A later Miocene deformation phase which resulted in uplift of the Southern and Central sub-basins in the inner part of the shelf and formation of a major sub-horizontal marine unconformity over these areas.

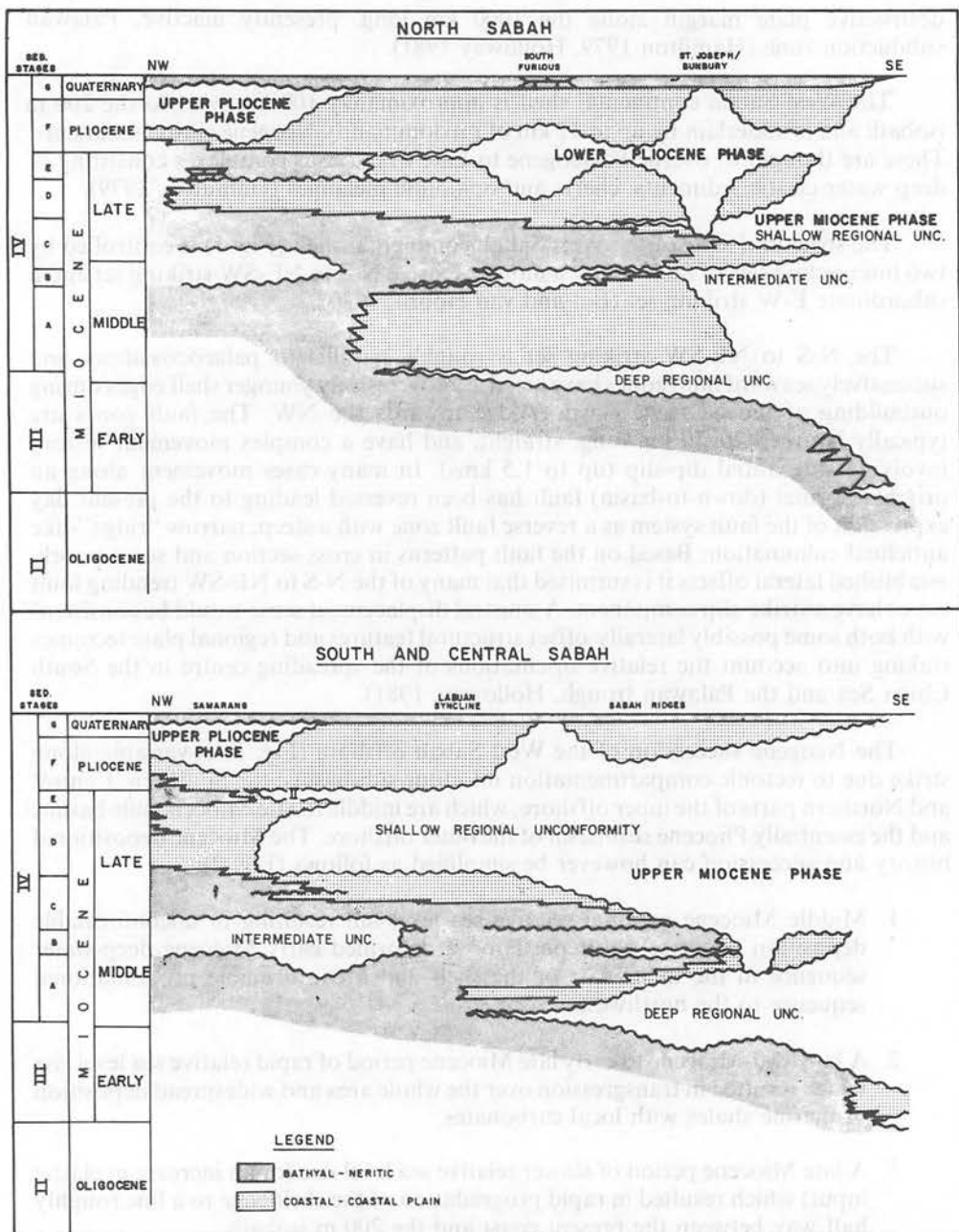


Fig. 2. West Sabah time stratigraphy. Due to syndepositional basement faulting the stratigraphies of the north, central and south sub-basins are different. The middle and late Miocene history can however be generalised as a transgressive—regressive "cycle". The slump scars described here were cut during the phase of rapid shelf progradation in the late Miocene.

This paper is concerned with the interaction of the rapid late Miocene progradation of the shelf edge with some of the major N-S or NE-SW striking fault zones. This resulted in the formation of tectonically unstable marine slopes which slumped to produce substantial quantities of turbidites and left behind dramatic slope unconformities as "slump scars".

DISTRIBUTION AND NATURE OF THE SLUMP SCARS

Slope unconformities interpreted as slump scars are scattered along virtually the entire length of the presently mappable late Miocene shelf edge (Fig. 3). In the south they are visible along a 30 km stretch of the N-S striking Morris fault. Northward is a gap of some 50 km due to poor seismic data. Slump scars re-appear along a 25 km section of the shelf edge SW of Pulau Mangalum however. Between P. Mangalum and the Erb West oil field the U. Miocene is poorly visible on seismic due to a thick Pliocene overburden. In the north slump scars are known along a continuous series of faults known as the Bunbury-St. Joseph and P. Mantanani Ridges for a distance of 90 kms.

Along the Morris fault and the Bunbury-St. Joseph/P. Mantanani Ridges the slump scars are clearly related to down-to-basin movements along fault zones. In the area SW of P. Mangalum the relationship is less clear, but a ridge is known from the immediate offshore which may also have been an active fault zone in the late Miocene.

Only the southern area along the Morris fault (Figs. 4-10) and the northern area, along the Bunbury-St. Joseph Ridge (Figs. 11-20) which lie within SSPC/Pecten's contract area will be described here.

The following evidence suggests that these unconformities are scars left by the downslope movement of large blocks of sediment in the form of slumps, slides, debris flows or turbidites:

1. They are only found within sequences displaying seismic foresetting (clinoforms) indicating a genetic relationship to a depositional slope (Figs. 5, 6, 12).
2. They can normally be shown to occur only in those parts of the progradational slope sequence adjacent to major fault lines.
3. The unconformities map out as shallow spoon-shaped scars. Some are more elongate but they generally widen rapidly seawards and do not have the elongate sinuous form of well developed canyons (Figs. 8, 9).
4. Bedding down-dip and above the unconformities differs from that up-dip and below. They are therefore not simple faults (Figs. 5, 6, 12).
5. Many unconformities are immediately overlain by seismically low amplitude relatively homogeneous units with seismic foresets (Figs. 5-7, 12-15). The unconformities cut into topset (shallower water) facies and therefore demonstrably resulted in a deepening. This has also been established from well penetrations of the unconformities.

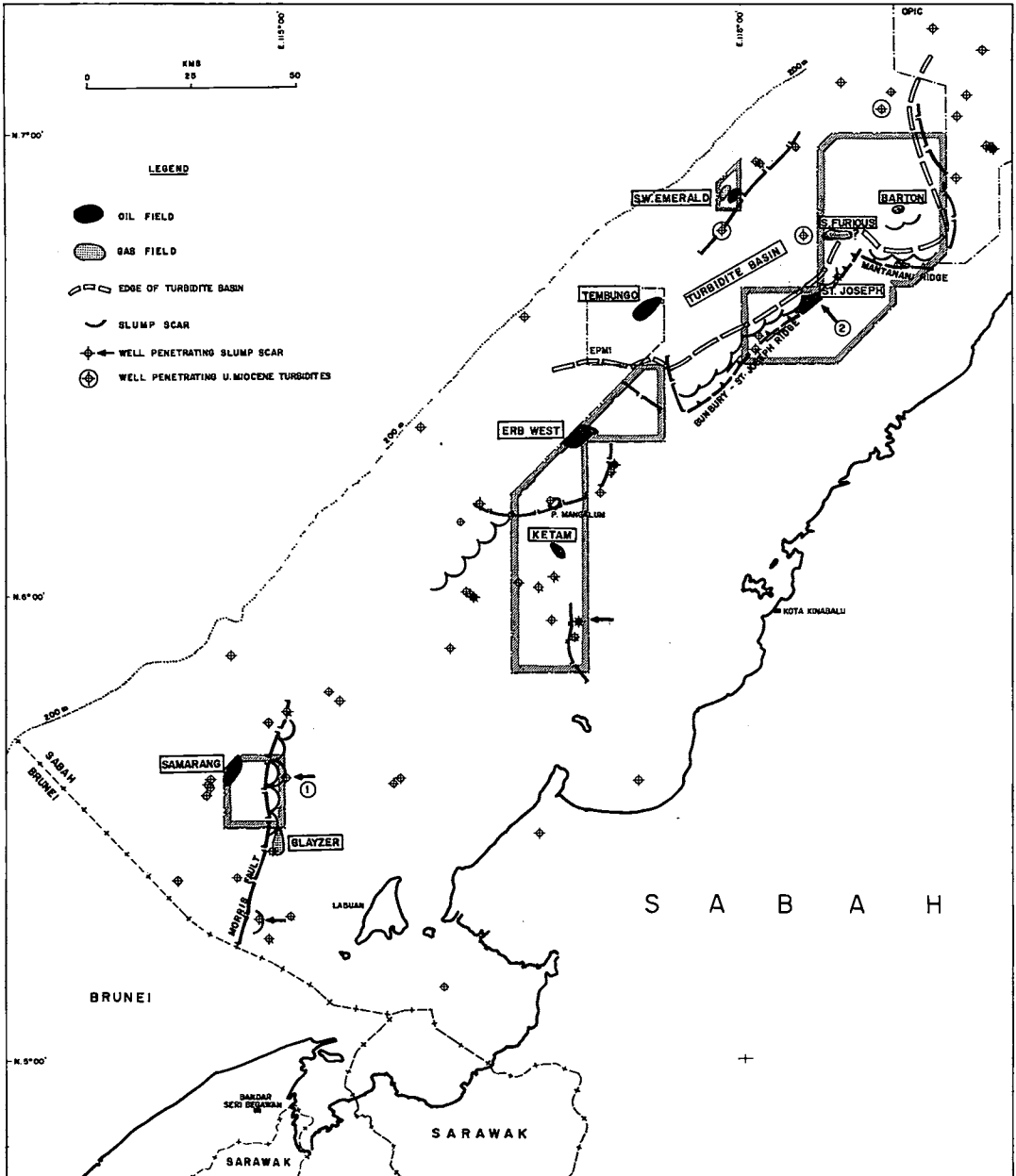


Fig. 3. Miocene/Pliocene slump scars offshore West Sabah. Slump scars are known from localities along the entire 250 km long late Miocene shelf edge. Slump scars east of the Samarang Oilfield (1) and southwest of the St. Joseph Oilfield (2) are described in detail in this paper.

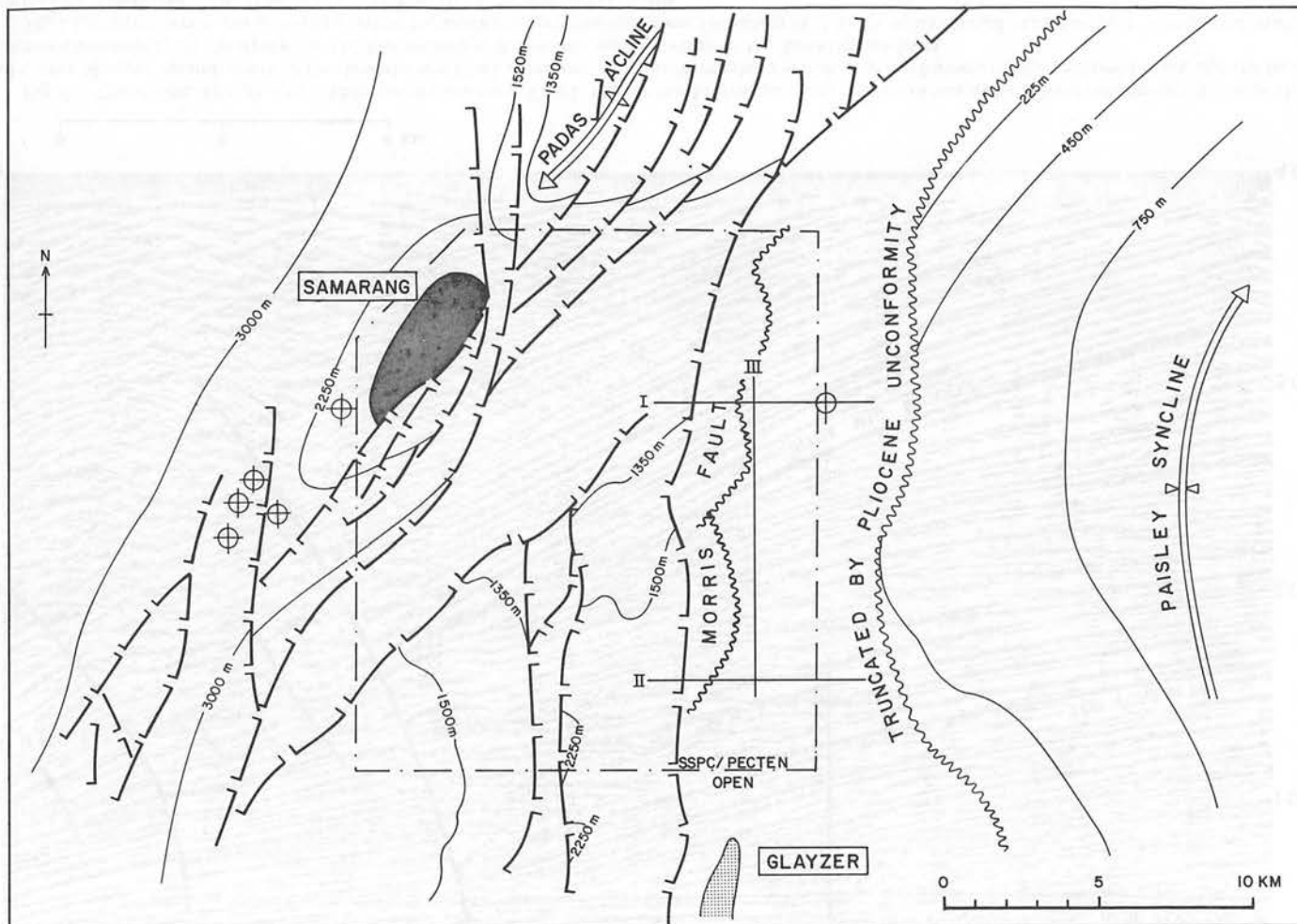


Fig. 4. Location map Samarang-Morris fault area. Westwards progradation brought the shelf edge to the Morris fault in the early late Miocene resulting in wholesale slumping towards the west. Seismic lines I, II and III are shown in Figs. 5-7 respectively and logs of the well on line I are shown in Fig. 10. For location of this map see Fig. 3.

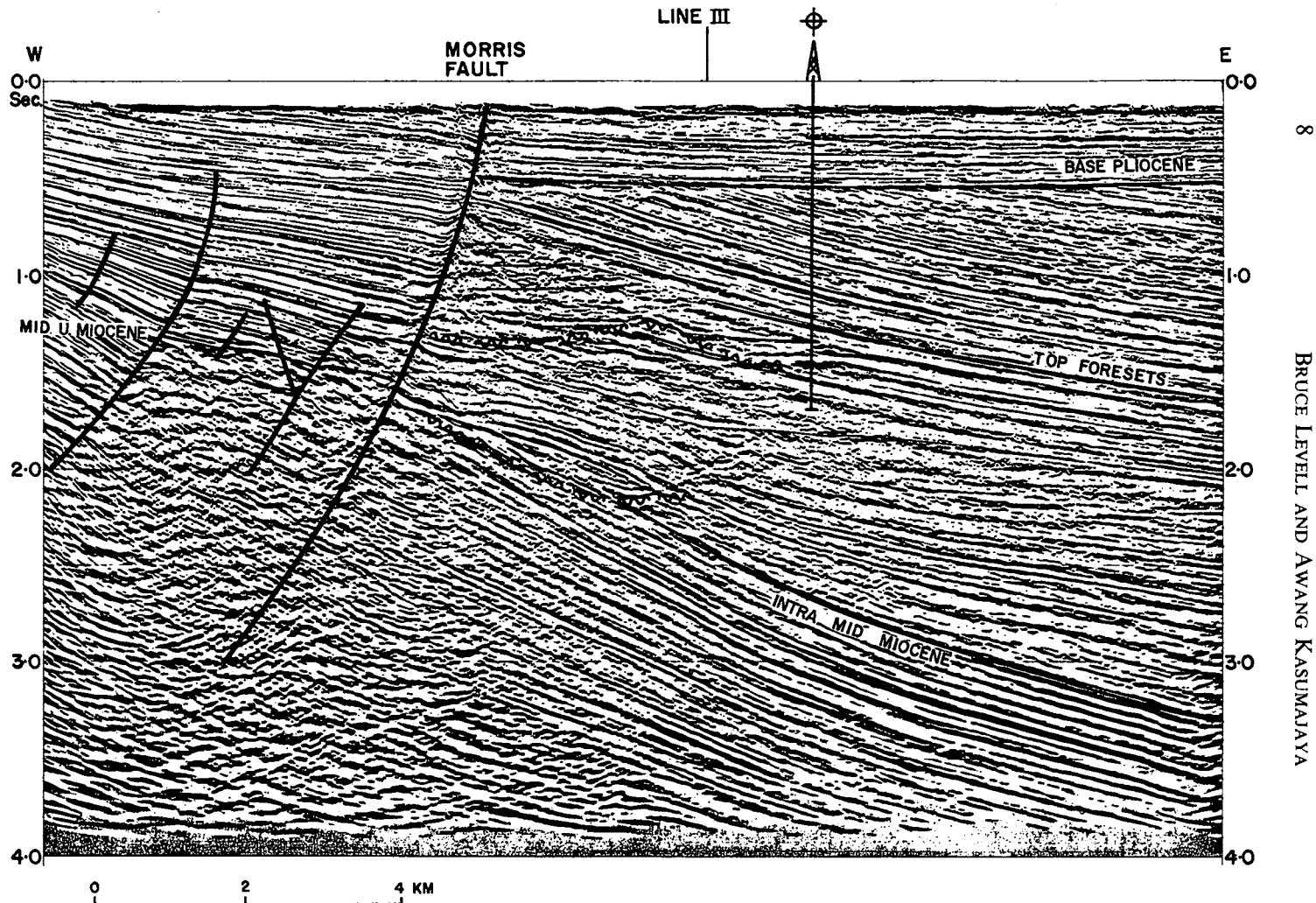


Fig. 5. Dip section through slump scars east of Samarang, Line I. The normal Morris fault separates two areas with different deformation histories: the mid Upper Miocene unconformity of the downthrown block correlates with a conformable horizon near top foresets on the upthrown block and the Base Pliocene unconformity of the upthrown block correlates with a conformable horizon in the downthrown block.

The local unconformity cut into, and overlain by, westwards-prograding seismic foresets at ca. 1.3 secs. is interpreted as a slump scar. This unconformity cuts into parallel-bedded topsets as has been demonstrated by the well (Fig. 10).

A deeper angular discordance at ca. 2.0 secs. is interpreted as a slide plane along which rigid body rotation of a large mass of base-of-slope (foreset) deposits has occurred.

The intra-Mid Miocene reflector is a downlap unconformity.

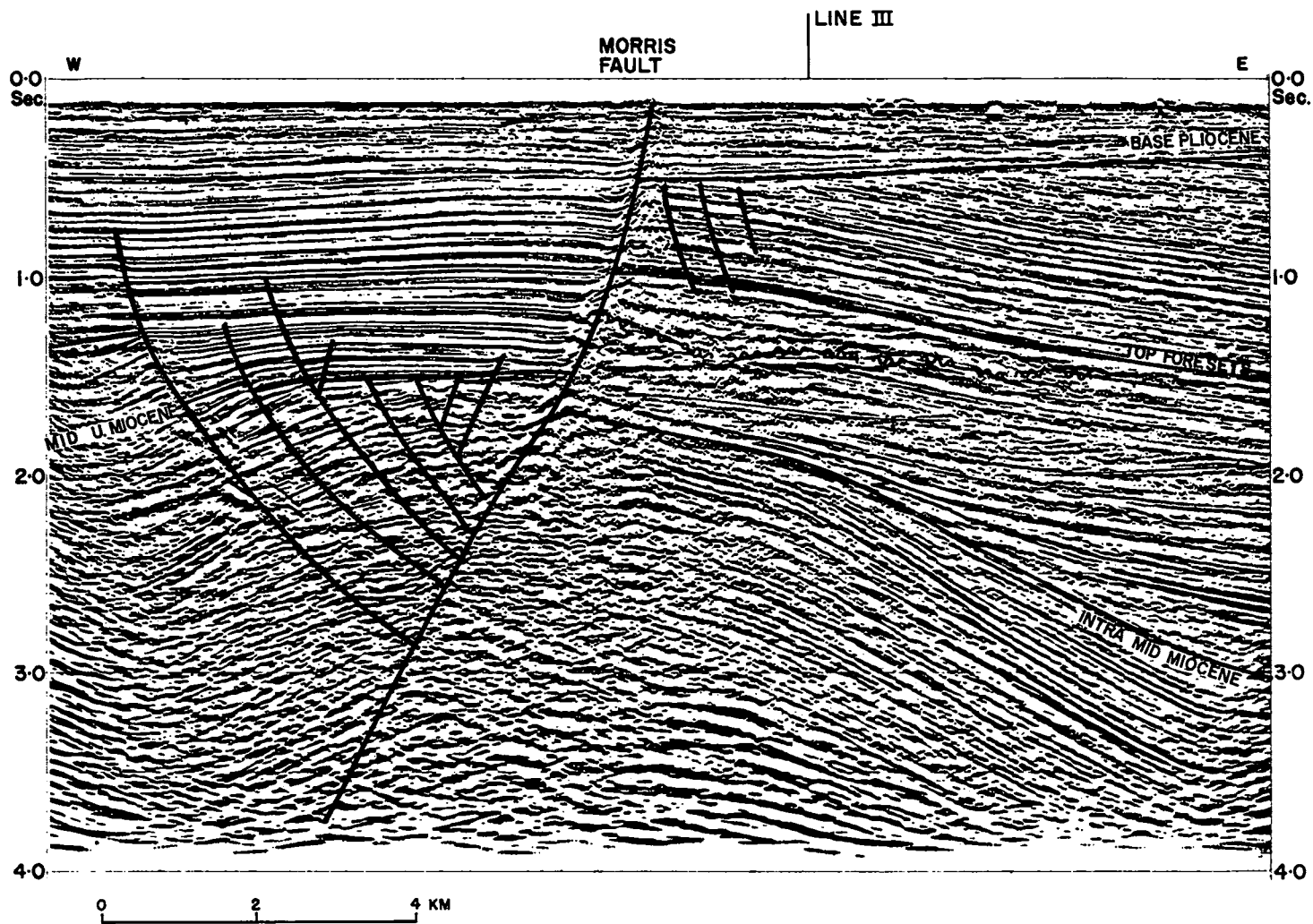


Fig. 6. Dip section through slump scars east of Samarang, Line II. For description see Fig. 5.

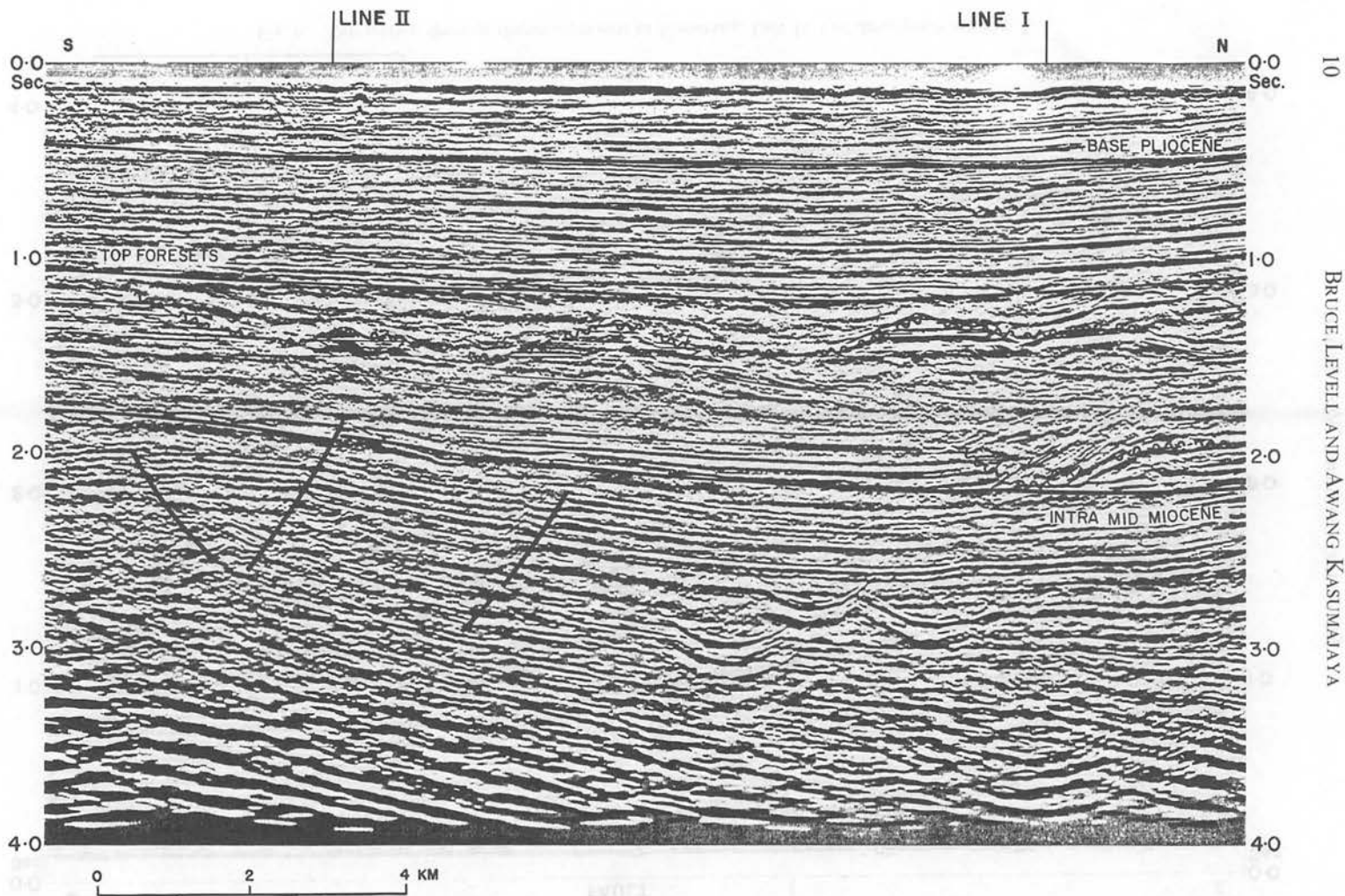


Fig. 7. Strike section through slump scars east of Samarang, Line III. Note that one single unconformity plane connects the slump scars of the dip lines I and II suggesting that the slumping all occurred in either one event or a series of events closely spaced in time. The rotated slide block of line I is again visible. The curved events at between 2.5 and 3 secs. are artefacts of the migration process.

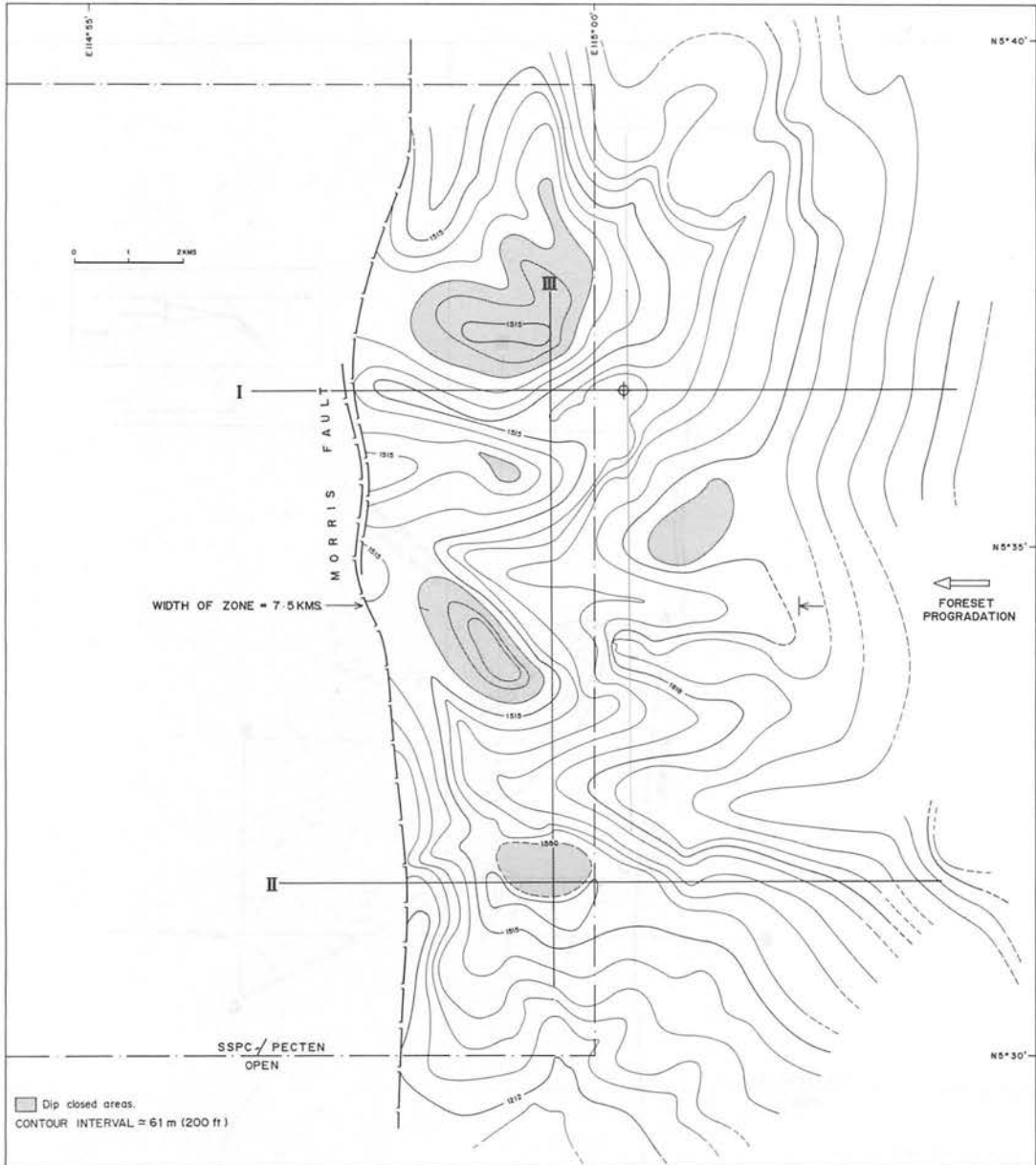


Fig. 8. Depth map Upper Miocene slump scars east of Samarang. This map of the slump scar unconformity of lines I-III and its laterally equivalent horizon to the east shows the regional eastward dip as well as the relief caused by slumping. Note the small closures in which remnants of topset deposits with potential reservoirs are overlain by the foresetted, clay-prone slump scar infills.

The slump scars cut back up to 7.5 km from the fault plane.

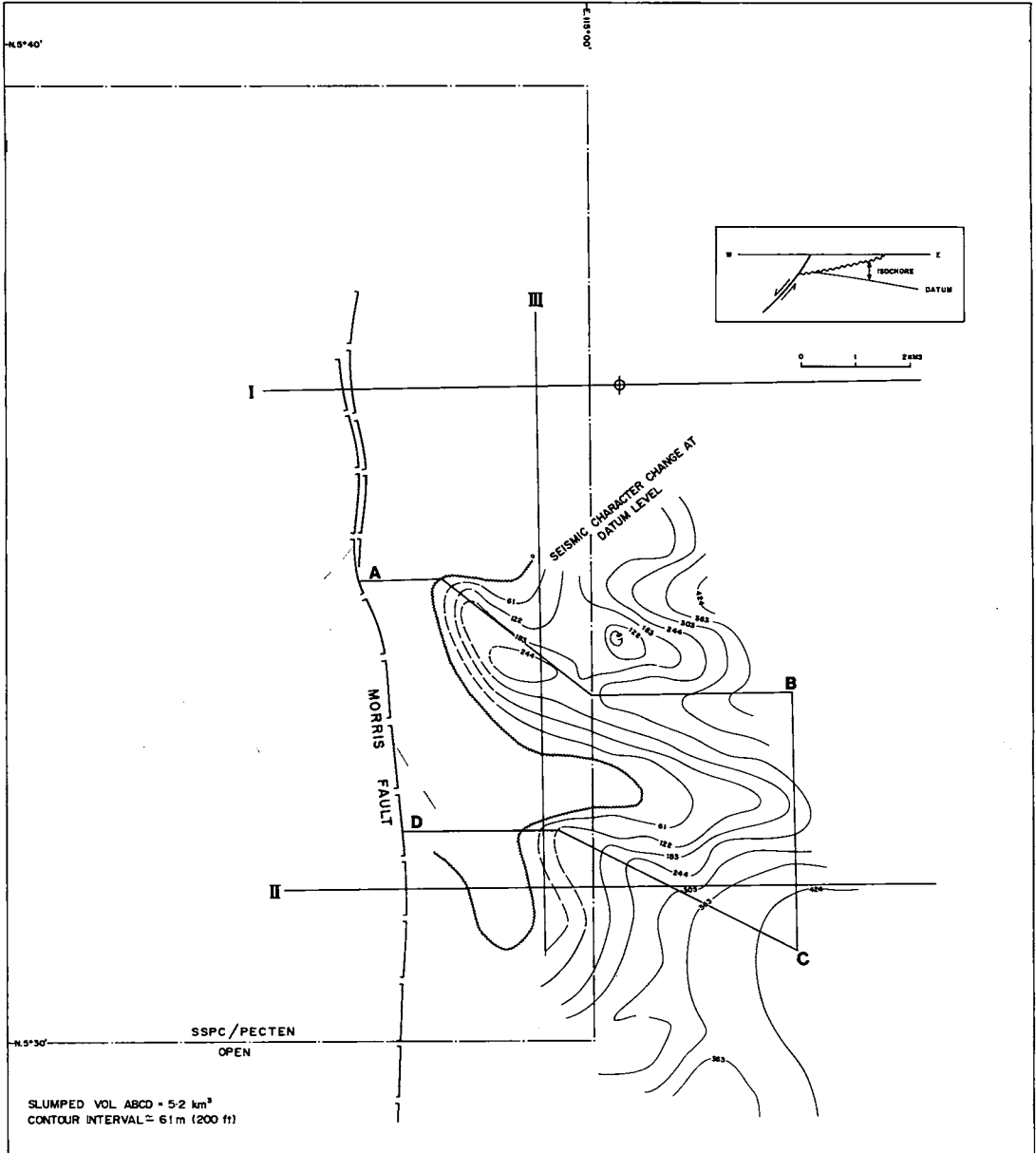


Fig. 9. Isochore map of section beneath slump scars east of Samarang. The slump scar morphology can be approximately reconstructed by making an isochore map based on a datum within the topset package below the unconformity as shown here.

6. In the northern area it can be shown that the laterally equivalent deposits basinward are turbidites which must have been derived from a slumping basin margin somewhere.
7. In two separate localities, rotated slump blocks can be seen resting on spoon-shaped slip planes (Figs. 5, 7). In both cases bedding has been rotated to dip back into the listric slump plane. The dimensions of these slump blocks are similar to those of the slump scars.

The dimensions of the larger slump scars and associated features are remarkably constant (Table 1). The slumped volumes ($1-5 \times 10^9 \text{ m}^3$) are comparable with those listed by Weser (1977). Smaller slump scars become individually indistinguishable as they pass into a "chaotic" or "channelled" seismic facies.

Seismic examples of similar dramatic slope unconformities have been recently published by Jaunich (1983) from offshore SW Africa.

TABLE 1
DIMENSIONS OF LARGER SLUMP SCARS

	SOUTH	CENTRAL	NORTH
Slump scar depth	425 m	500 m	600 m
Slump scar width	1-2 km	1.5-2 km	2-5 km
Slump scar volume	e.g. 5.2 km^3	?	e.g. 1.5 km^3
Slump scar maximum slope angle	19°	26°	27°
Foreset height in undisturbed section*	520 m	350 m	330 m
Foreset average slope angle in undisturbed section*	6°	5°	13°**
Foreset height in slump scar infill*	520 m	200 m (min)	300 m
Foreset average slope angle in slump scar infill	12°	6°	21°
Width of slump scar zone	7.5 km	7 km	5 km (min)

* Undecomacted: Overburden 1.2-2.1 km

**Undecomacted: Overburden 0.3-0.6 km

REGIONAL DESCRIPTION OF UPPER MIOCENE SLUMP SCARS

Southern area

The slump scars in South Sabah are restricted to the area immediately east of the Morris fault (Figs. 4-8). This normal fault has a downthrow of up to 1.1 km at the level of the Upper Miocene unconformity, and a growth index of approx. 2 for the Pliocene section. The fault became active during the late Miocene and continued activity into the Pleistocene.

The slump scars cut into both the seismic foresets of the prograding slope sequence and into about 200 m of overlying parallel-bedded topsets (Figs. 5-7). The

latter have been shown by drilling to be sand-bearing, terrestrial to coastal deposits (Fig. 10). It is therefore probable that the coastline itself had prograded as far as, or even beyond, the Morris fault before instability and slumping resulted. Possibly progradation of the clastic wedge across the fault zone triggered movement along some pre-existing basement weakness.

The slump scars approximate spoon-shaped scoops flaring towards the west. There was also however some slumping of material in N-S and S-N directions resulting in erosion of the high divides between adjacent scars. The net effect was to produce separated erosional remnants of sand-bearing topset deposits between coalescing slump scars. Some of these remnants have closed structural contours at the slump scar unconformity level. If the deep water claystones of the slump scar infill are an effective seal to hydrocarbon migration then the erosional remnants represent potential stratigraphic traps. A well drilled in the southern area in 1972 was specifically designed to test this hypothesis (Fig. 10). It found a 200 m thick coarsening-upward claystone-siltstone succession above the slump scar but only found traces of gas in the reservoir section below the unconformity. A second well drilled further south also penetrated a clay-filled slump scar behind the Morris fault (Fig. 3).

Volumes calculated from the isochore map of the interval between the unconformity itself (Fig. 9) and a datum beneath the unconformity suggest that some 25 cubic km of sediment were re-deposited by gravitational processes into deep water west of the Morris fault along the 20 km of the fault that is depicted on Fig. 8 (1.25 cubic km per fault-km). An estimate, based on the single well which penetrated the slumped section in the centre of the mapped area, suggests that the sand/shale ratio of the whole slumped section (topsets and foresets) is approximately 30%. This implies that approximately 0.4 cubic km of sand per fault km should exist in the form of turbidites on the downthrown side of the fault (e.g. 40 m over an area of 10 sq. km).

To date the time equivalent section of the slumped units has not been penetrated on the downthrown side of the Morris fault.

Interesting, but unresolved, questions concerning the slump scars include the following:

1. Whether the Morris fault actually formed a submarine scarp, or merely initiated slumping due to seismic triggering of sediment instability on the depositional slope of the foresets? The restriction of the slump scars to a strip 7 km wide behind the Morris fault is perhaps due to both factors.
2. Whether the individual scars formed during single events or during a series of slump events? Possibly the slumping took place as a series of retrogressive (headwater-retreating), progressively smaller slumps as has been documented from recent slumps (e.g. Andresen and Bjerrum, 1976).
3. Whether or not all the slump scars formed at the same time? Strike sections do not show clear intersections of adjacent slump scars (e.g. Fig. 7) that would be indicative of an age sequence. It is therefore possible that wholesale slumping

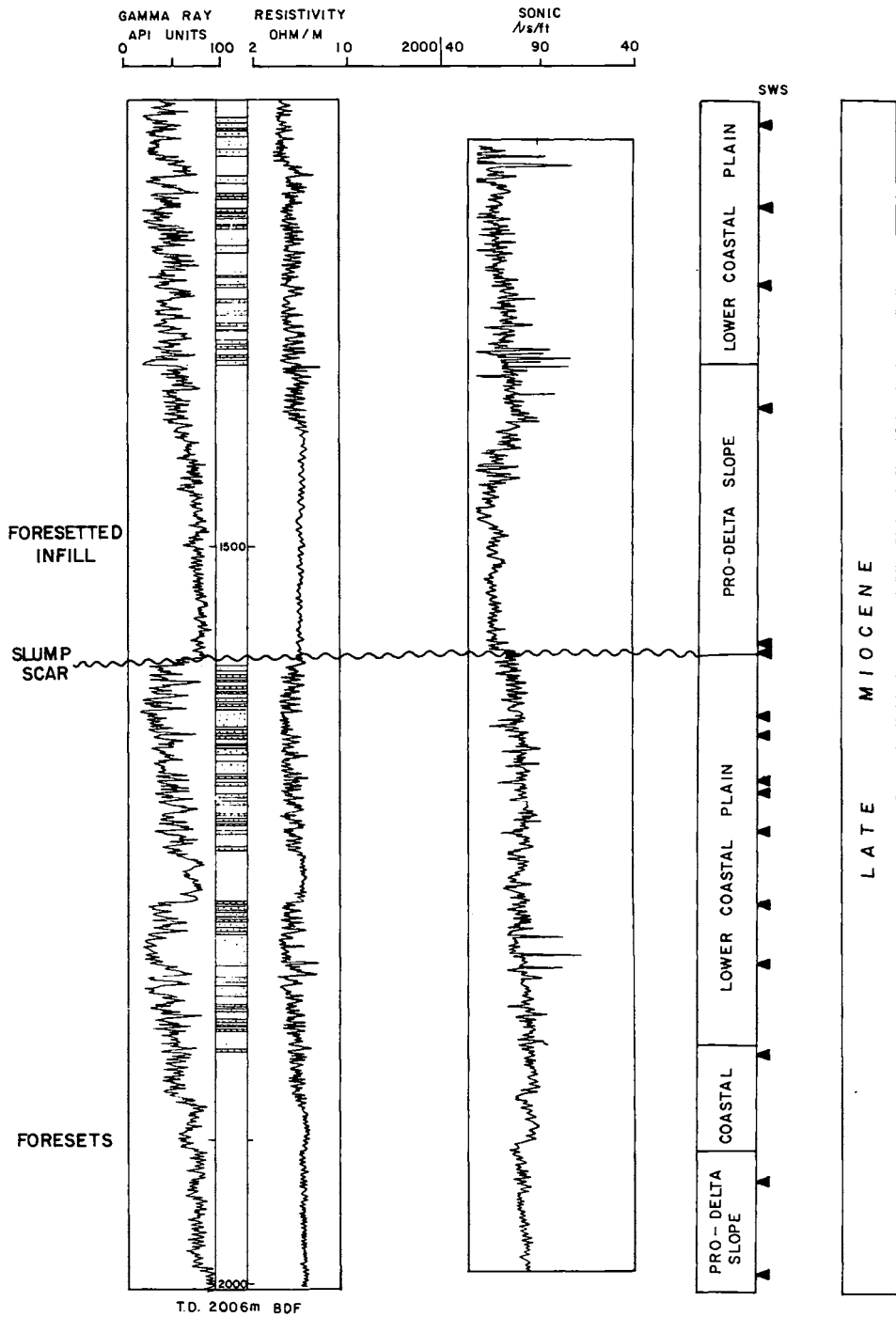


Fig. 10. This well, located on Line I (Fig. 5) penetrated the deeper unit of seismic foresets and overlying reservoir-bearing topsets, into which the slump scar has been cut, as well as the seismically foresetted infill. The well proved that the latter is a thick shale and hence a potential top and lateral seal.

occurred at once. The deeper rotated slump block of Figs. 5 and 7 is however clearly a separate, earlier, event.

4. To what extent is the morphology of the slump scars purely due to slumping or does it include some post-slump modification by turbidity current erosion? The lack of sand at the base of the slump scar infill in the well does not necessarily imply lack of turbidity current activity since the slump scars could have acted as zones of sedimentary bypass. The relatively simple smooth shapes of the scars, the lack of tributary systems (Fig. 9) and the lack of 'overdeepening' suggest that they are essentially unmodified slump scars. This is possibly due to a high rate of relative sea level rise in the post-slumping period reflected in topset aggradation rather than a downward shift in coastal onlap.

Northern area

In contrast with the Morris fault, a single normal fault which resulted in simple slope instability and the incision of slump scars landward of the fault, the Bunbury–St. Joseph Ridge (Fig. 3), was, during the late Miocene, a rotating, seaward-dipping, flank above a buried fault zone. The slump scars along this trend are found seaward of the intensely faulted crest of the ridge and formed on the flank as this was progressively rotated to dip northwestwards (Fig. 11).

Also in contrast with the southern area, slumping continued for a relatively long period of time, with a section of some 2 km total thickness being involved in repeated slump events (Figs. 12–15). This longer duration of slumping can perhaps be attributed to the gradual rotation of a flank rather than sporadic, infrequent, large movements on a fault.

As in the southern area however the slump scars cut back deeply into parallel-bedded topset deposits. These do include some sand (particular intervals have sand percentages as high as 25%) but have been shown by several well penetrations to be predominantly composed of shallow marine claystones and silts. This is somewhat surprising in view of the high amplitude continuous seismic facies.

Palaeogeographically, well data indicate that the coastline was probably just on the landward (SE) side of the ridge and that a narrow shallow marine shelf extended across the ridge. Oversteepening on the seaward (NW) side of the ridge led to slumping. The progradation of the shallow marine shelf (topsets) and the cutting of slump scars alternated in both time and space. This is clearly shown by the fact that the base of each remnant topset package, above a slump scar fill and beneath the coalescing younger slump scars, is at a different stratigraphic level and cannot be correlated by a phantom horizon (Figs. 12–15). In plan view the basin margin was probably both scalloped and lobate with alternating destructional slump scars and constructional areas (Fig. 16).

Slump scar infills show seismic foresetting (Figs. 13–15). Interestingly these foresets do not have dip azimuths normal to the strike of the ridge but tend to indicate more northerly progradation (they are visible on both 'dip' and 'strike' lines). This is taken as evidence for the existence of a culmination on the ridge towards the south with a northeastward plunging axis.

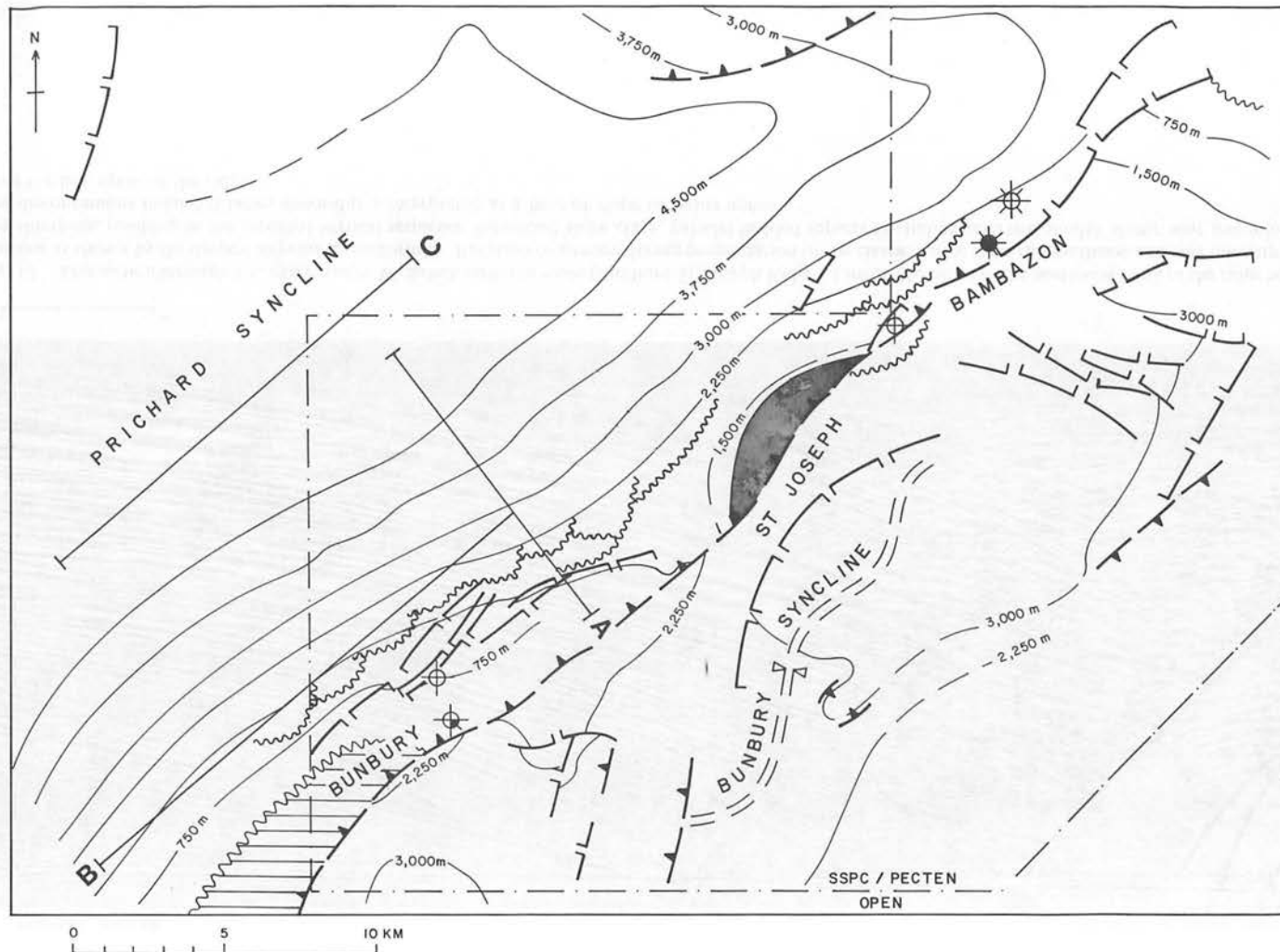


Fig. 11. Location map Bunbury-St. Joseph Ridge. The Bunbury-St. Joseph Ridge (for location see Fig. 3) differs from the Morris fault system in that it was a zone of steep westward down-bending rather than a single fault line. The ridge was strongly uplifted in the Pliocene with the southeastern flank locally reverse faulted over the Bunbury syncline block to the southeast.

The slump scars are to be found largely on the northwestern flank of the ridge and their lateral equivalents, turbidites, were deposited in the turbidite basin indicated on Fig. 3, which includes the Prichard syncline.

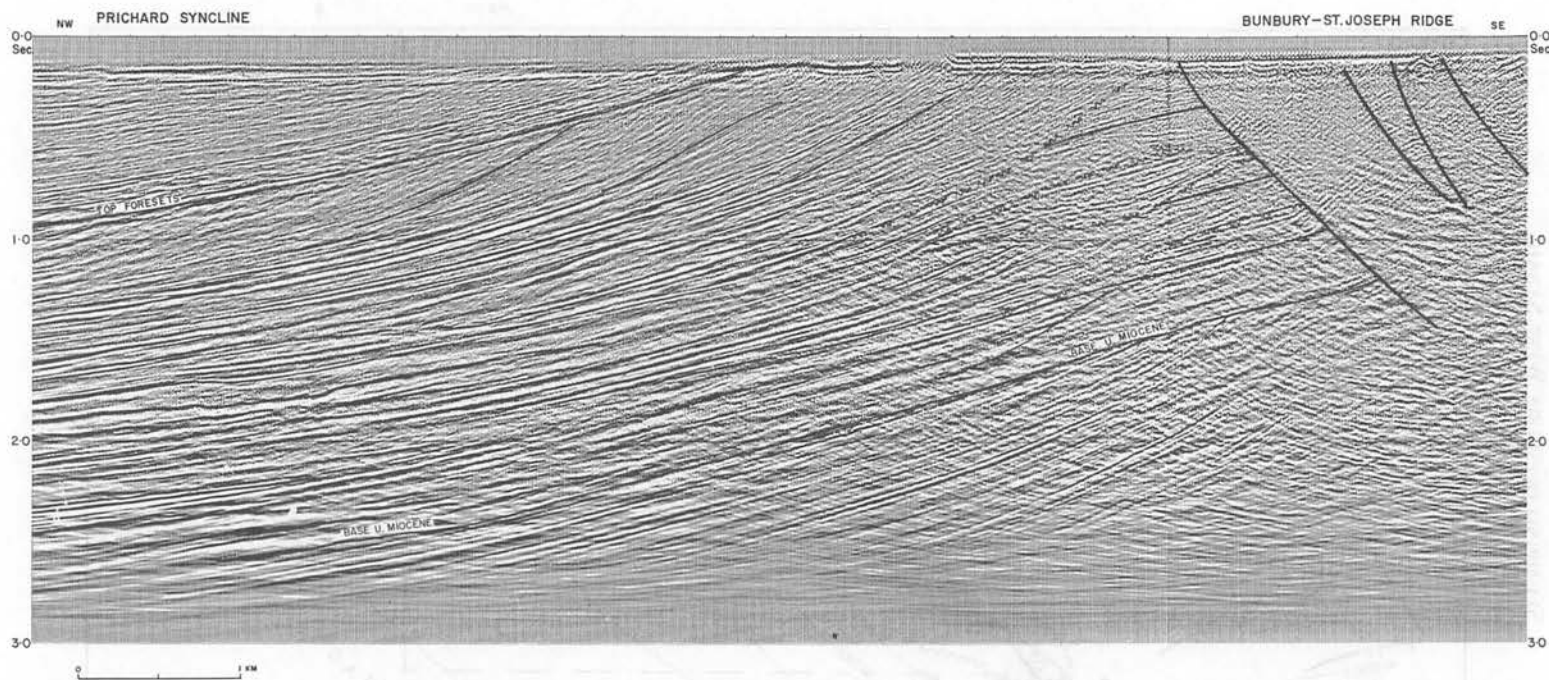


Fig. 12. Dip section through S.E. margin of N.W. Sabah turbidite basin (Bunbury-St. Joseph Ridge), Line A. Rotation of the northwest flank of the ridge began in the late Miocene as shown by the deepest angular unconformity. Rotation continued during progradation of the clastic wedge from the southeast and was interrupted several times by slumping, resulting in the repeated vertical sequence; foresetted slope clays, parallel bedded topsets (including reservoir sands); slump scar unconformity. The discontinuous mounded facies down-dip is interpreted as a base of slope turbidite apron. Note the late uplift of the ridge.

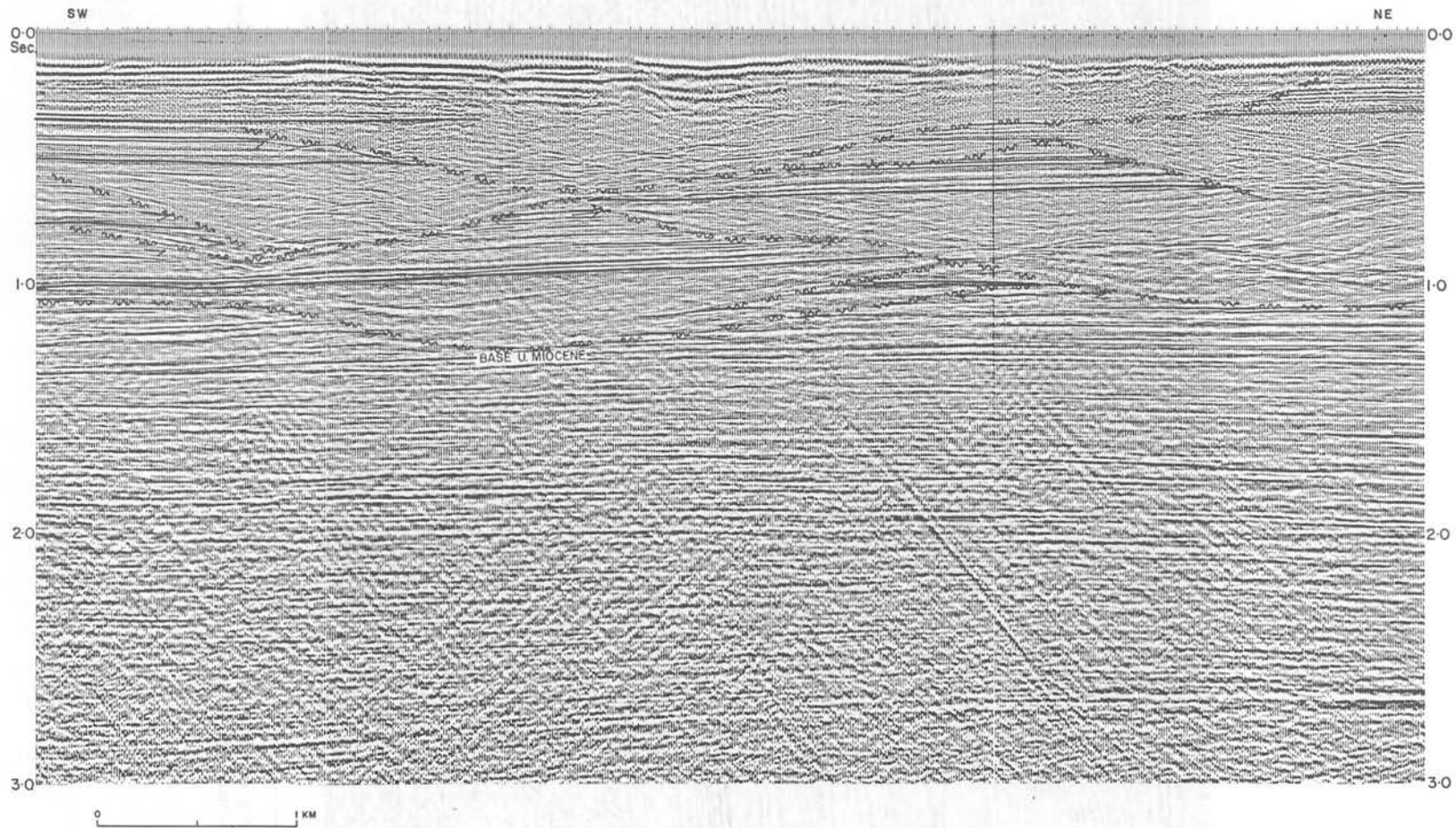


Fig. 13. Strike section SW of St. Joseph, Line B (Part 1). Note the lenticular remnants of parallel bedded topsets resting on weakly reflective (or faintly foresetted) slope deposits and cut into by coalescing slump scars. These lenses represent potential stratigraphic traps.

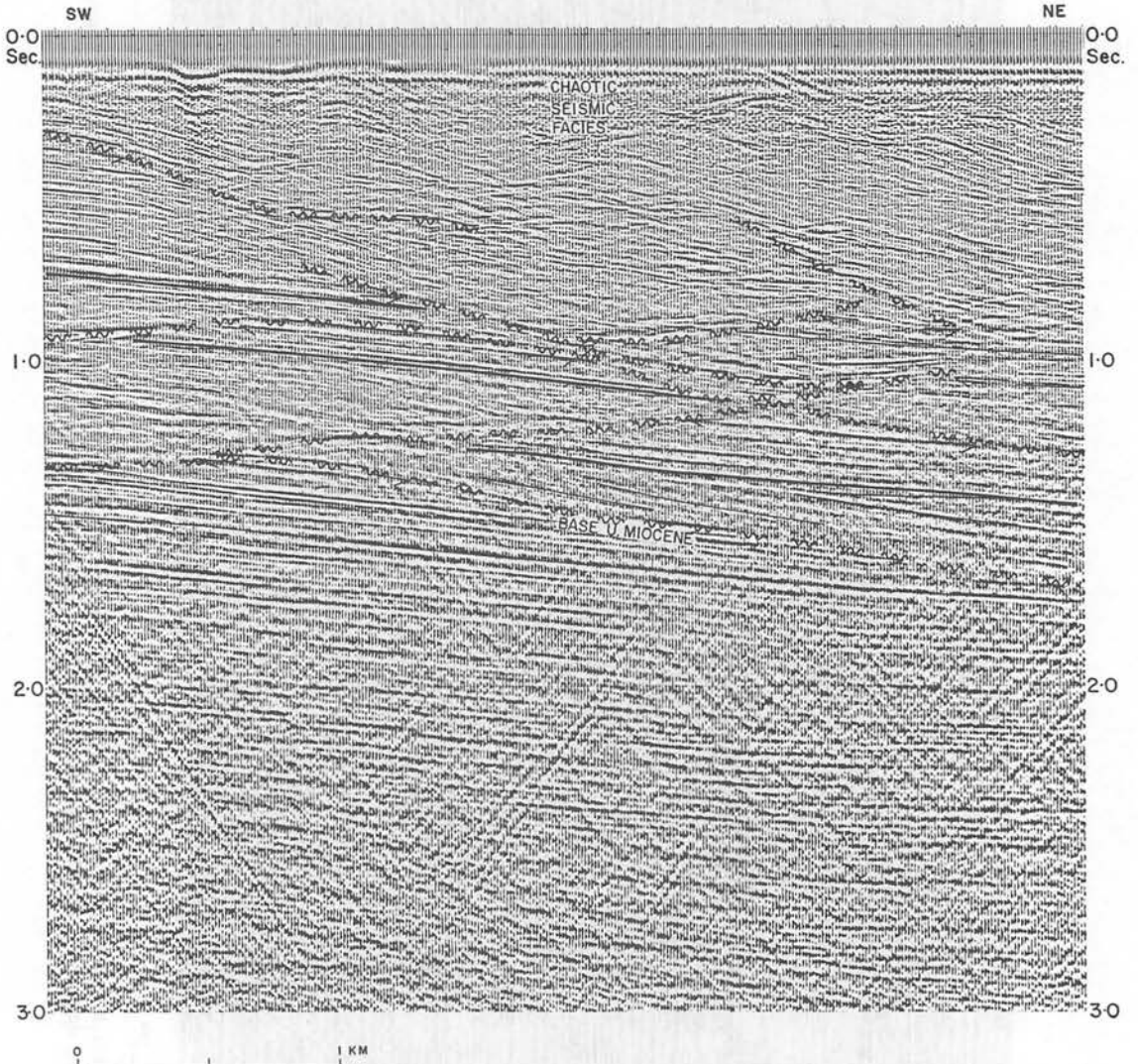


Fig. 14. Strike action SW of St. Joseph, Line B (Part 2). As in Fig. 13 note that in the shallow section individual slump scars appear to be smaller and can no longer be separated from one another.

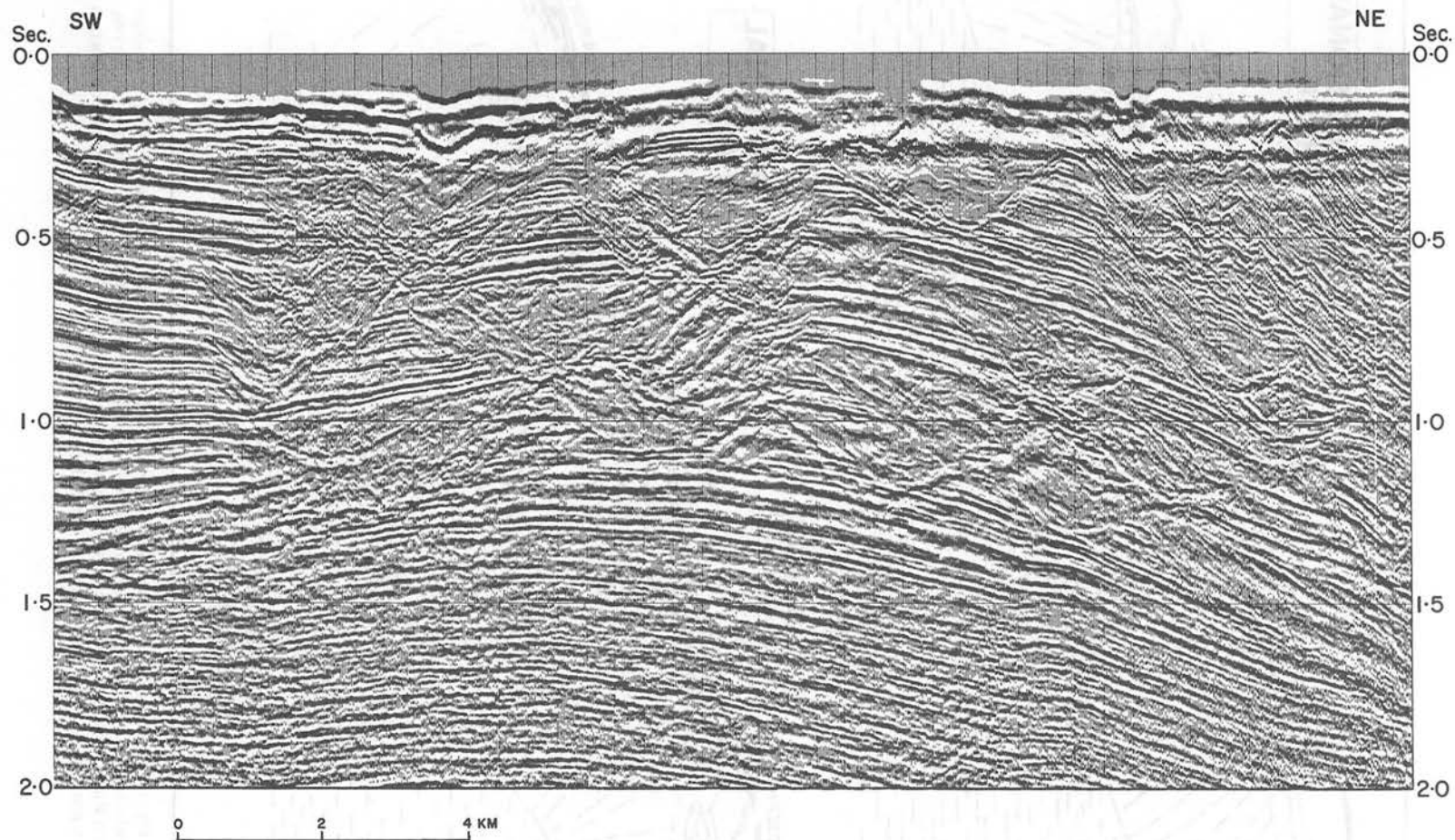


Fig. 15. Strike section S.W. of St. Joseph (Squeezed) Line B. In this section the horizontal scale of Figs. 13 and 14 has been reduced to give a clearer view of the slump scars.

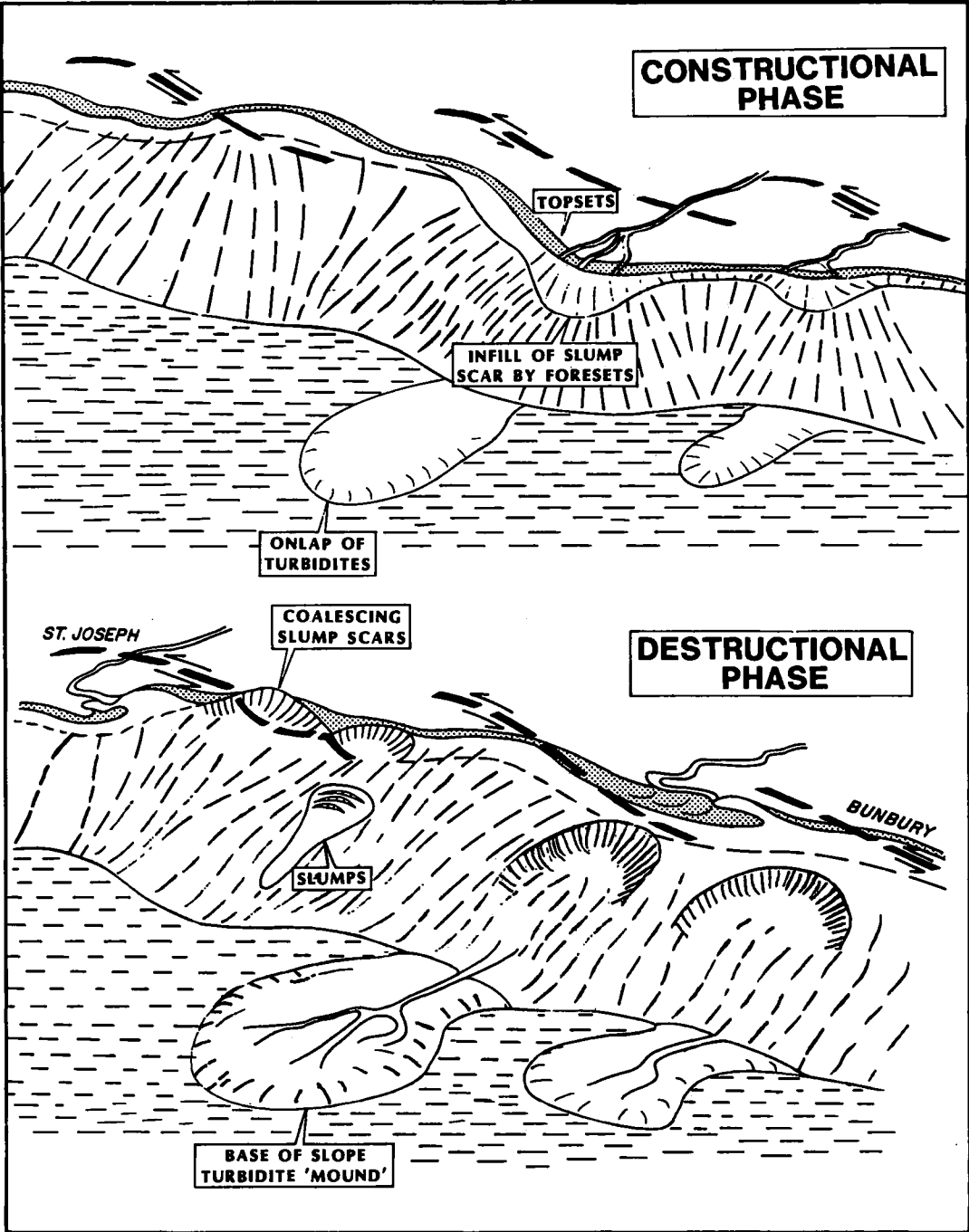


Fig. 16. Schematic evolution of slump scars on Bunbury-St. Joseph Ridge. In contrast with the single unconformity of the Morris fault slump scar, a stacked series of slump scars is visible along the Bunbury-St. Joseph Ridge. This view, from the north, illustrates the alternation of slope construction and destruction which probably varied in both time and space along the ridge.

Locally, slump scars of smaller size were formed resulting in a chaotic channelled seismic facies in which individual slump scars can no longer be defined on conventional seismic sections (Fig. 14). Probably this indicates a shorter time period between individual slumps perhaps related to local increases in rotational subsidence of the flank or in sediment supply rates.

Towards the St. Joseph oil field a few major slump scars can be shown to amalgamate to form a single planar unconformity. This feature is difficult to explain but could represent the tangent to a series of headward-retreating slope failure envelopes (Andresen and Bjerrum, 1976).

Well correlation within the St. Joseph Field (Figs. 17, 18) illustrates that packages of shallow marine reservoir-bearing topsets are separated by an unconformity with relief of up to 100 m overlain by shales. Locally, sequences with chaotic dips have been found within the shale infill of this unconformity which, in the light of the seismic evidence, is also interpreted as a slump scar. This feature has only about one quarter of the relief of the examples shown in Figs. 12–15 and is not visible on conventional seismic sections.

Down-flank of the slump scar belt, which has a minimum width of 5 km (the proximal parts are eroded), is a complex seismic facies which onlaps the base of the slump scars and is partially downlapped by prograding seismic foresets. This seismic facies has basically discontinuous reflectors of variable amplitude some of which are convex-("mounded" Figs. 12, 19, 20). It underlies prograding foresets of latest Miocene age and is interpreted as the seismic response of turbiditic bottomsets. This interpretation is strengthened by the penetration of sands with deepwater faunas interpreted as turbiditic in two wells drilled into lateral equivalents of the mounded seismic facies further offshore (one well is illustrated in Fig. 18). The turbidite section is up to 1.8 km thick and includes up to 500 m of net sand. The turbidite basin had a minimum area of 3000 sq. km. (Fig. 3).

The interbedding of turbidites, prograding foresets and slump scars cut into shallow marine topsets (Figs. 12, 18) on the NW flank of the Bunbury—St. Joseph Ridge gives a detailed picture of the complexities to be expected at the edge of a turbidite basin. This is often an area which is destroyed by continuing tectonic movements of the basin margin.

Interesting points concerning this turbidite basin margin are the following:

1. The 'mounded' seismic facies dies out away from the foot of the ridge and clear mounds are no longer discernible at distances of more than 20 km from the ridge. Although the mounds are probably indicative of sandy turbidite lobes, lack of mounds clearly does not mean that the turbidites are not sandy since two well penetrations have reasonable amounts of sand (500 m and 80 m) in areas where the bottomset seismic facies is continuous—parallel.
2. The individual mounds are distributed randomly along strike and do not coalesce to form a major fan body. This is probably due to the linear nature of

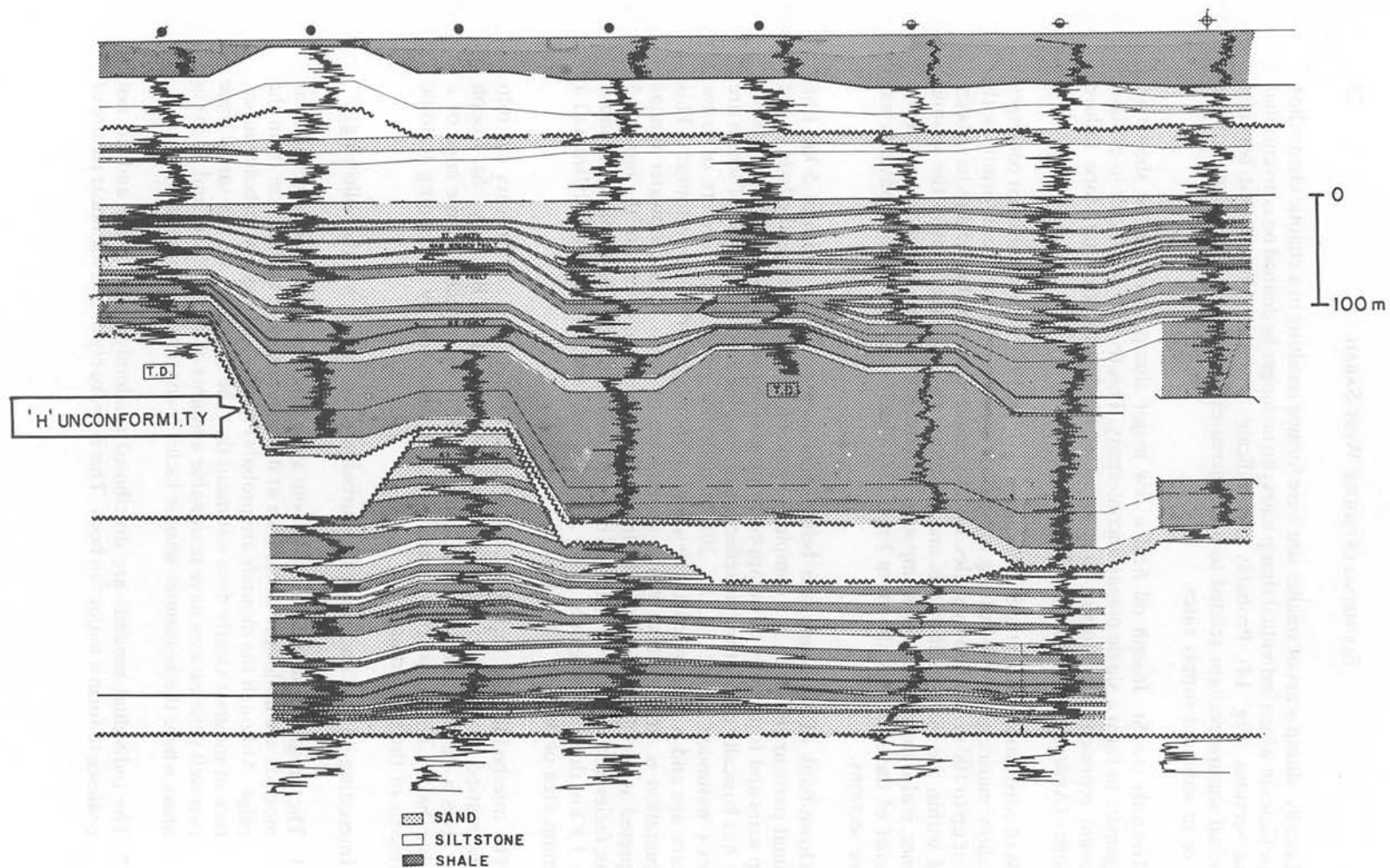


Fig. 17. This well correlation panel, which is more or less a strike section through the St. Joseph Field (Fig. 11) illustrates the same geometry as Figs. 12-15. Note that the slump scar unconformity ('H' unconformity) has a relief of only about 100 m which is less than one-quarter of that of the slump scars demonstrated on the seismic sections. The 'H' unconformity is not visible on conventional seismic data.

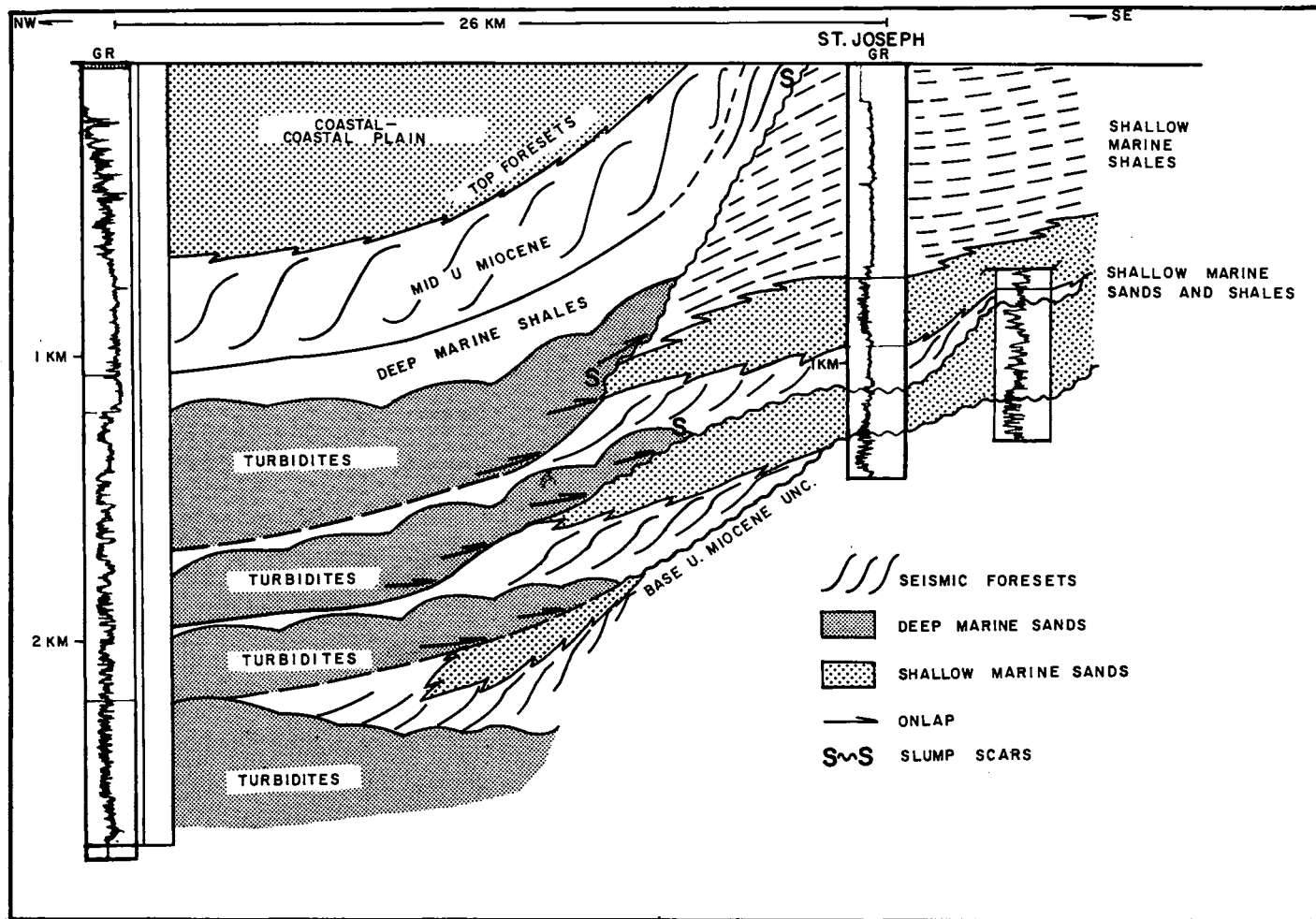


Fig. 18. Schematic geological cross-section N.W. Sabah turbidite basin. A well drilled in the NW Sabah turbidite basin on the northwestern flank of the Prichard Syncline (Figs. 3, 11) encountered 500m of net turbidite sand in the Upper Miocene. This contrasts with only about 60 m of net sand in the shallow water (topset) packages of the St. Joseph Field and suggests considerable by-pass of sand through the Bunbury-St. Joseph slope system into the NW Sabah turbidite basin.

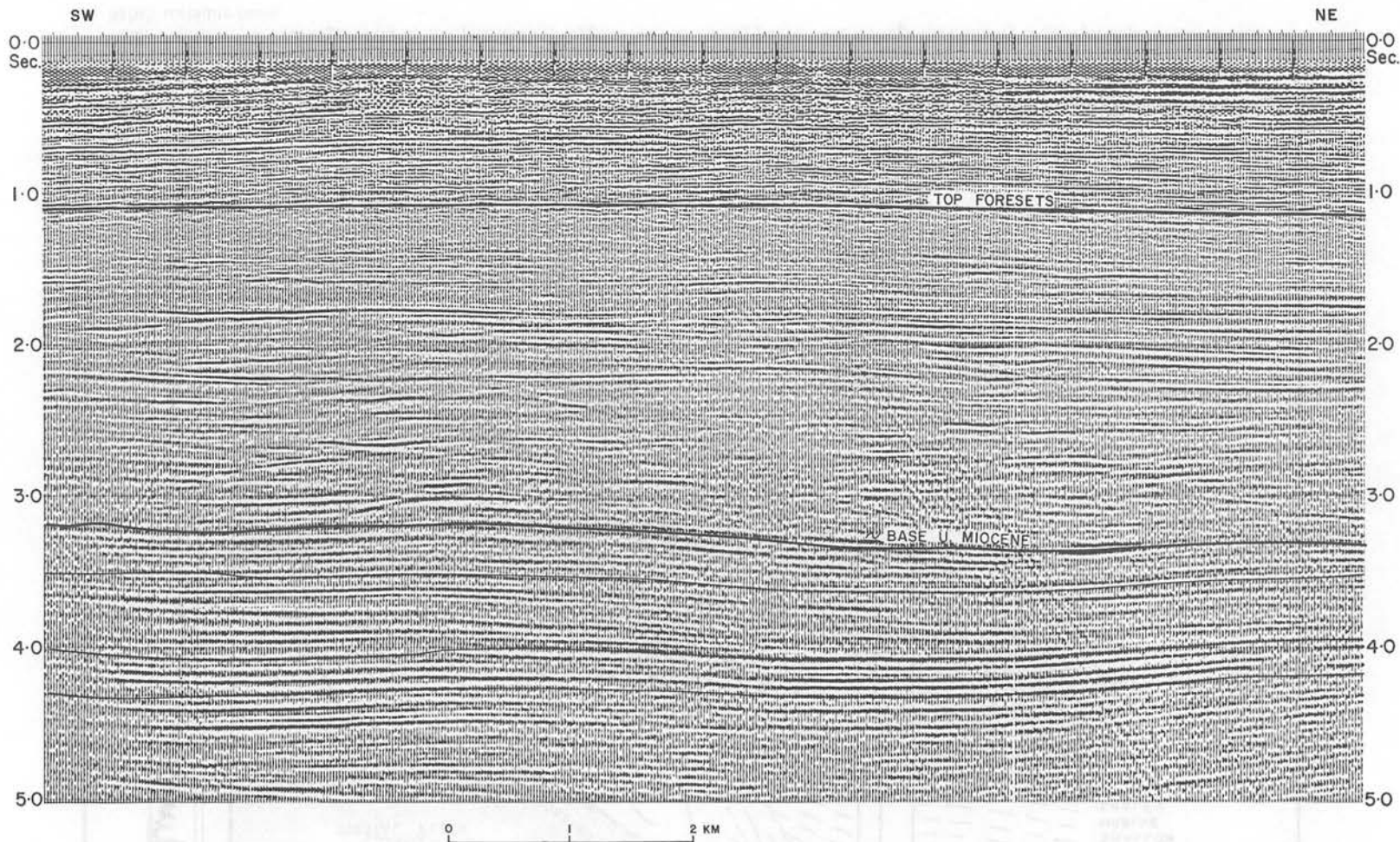


Fig. 19. Strike section through N.W. Sabah turbidite basin, Line C. This line (for location see Fig. 11) illustrates the characteristic mounded-discontinuous seismic facies which has been shown to represent sand-prone turbidites. The scattering of slump scars along the 77 kms long Bunbury St. Joseph ridge led to deposition of a series of overlapping turbidite lobes rather than a single, organised, deep sea fan.

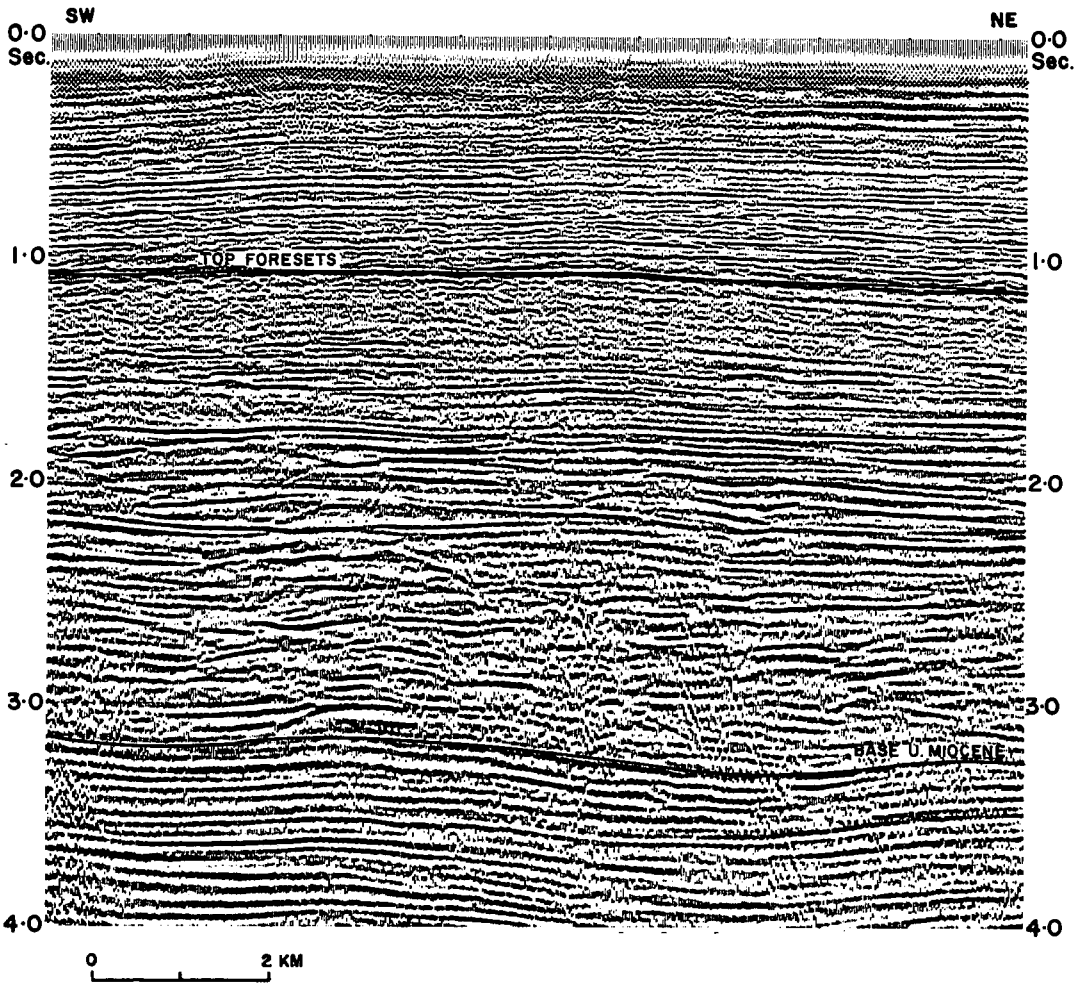


Fig. 20. Strike section through N.W. Sabah turbidite basin, Line C. The horizontal scale of Fig. 19 has here been reduced to illustrate the mounded-discontinuous seismic facies more clearly.

the sediment input, along the 70 kms of the Bunbury–St. Joseph ridge as opposed to input from a discrete point source. Deep sea fan models are probably not applicable to these turbidites, which were derived from a ‘gullied’ margin (Haner and Gorsline, 1978).

3. The sand/shale ratio of some of the turbidite sections is higher than that of the average topset sections which are incised by the slump scars. This indicates sedimentary by-pass of sand through the slump scars and/or concentration of the sand fraction of the turbidity currents in particular areas with the fines being efficiently segregated elsewhere.

SEA LEVEL CHANGES

The controlling factor on the formation of the Upper Miocene slumps discussed above is quite clearly the progradation of a shelf/slope system across active fault zones. It is striking however that the late Miocene slope system in particular demonstrates such fine examples of slumping. Isolated slump scars are indeed known from middle Miocene and Pliocene slope systems offshore West Sabah but these are by no means as extensive as those of the late Miocene.

In part this is due to the situation of the SSPC/Pecten contract area with respect to the shifting palaeogeographic picture. The Pliocene shelf edges are further offshore whereas the middle Miocene shelf edge is generally deeply buried or has been subsequently tectonised and is therefore not clearly displayed on seismic lines.

The late Miocene was however a time of rapid progradation with widespread seismic foresetting offshore West Sabah. Possibly the widespread occurrence of slumping at this time is ultimately due to this extensive progradation (Fig. 2) which brought the clastic wedge to the various fault zones (Fig. 1). This regressive episode could be due either to increased clastic input or a slower rate of relative sea level rise. A reduction of the rate of relative sea level rise is favoured since the major earth movements of the late Miocene post-date the formation of the slump scars. According to Vail *et al.* (1976), the late Miocene did see two important global relative sea level falls. The limited age control on the West Sabah slump scars would relate them to the early late Miocene rather than the later late Miocene Messinian event.

CONCLUSIONS

1. The late Miocene of West Sabah displays fine examples of slump scars cut into clastic depositional slopes above fault zones.
2. These slumps provided sand along a "gullied margin" for thick sequences of sandy turbidites deposited offshore.
3. The slump scar infills so far penetrated by the drill have been shown to be shaly and potential top/lateral seals.
4. Erosional remnants of topsets between slump scars represent possible stratigraphic traps.
5. The widespread occurrence of slumps in the late Miocene is due largely to the presence of syndepositional linear fault zones with large throws but possibly also to sea level fall resulting in progradation of the sedimentary system on a broad front to reach these fault zones.
6. This particular set of circumstances favouring the widespread occurrence of slumps cut into sand-bearing topset deposits may be characteristic of destructional plate margins with a strike-slip component and a high rate of clastic input. Other examples might include the Great Valley sequence (Palaeogene) of California

(Armstrong, 1978; Garcia, 1981) and the modern continental margin of the California borderland (Haner and Gorsline, 1978).

ACKNOWLEDGEMENTS

This paper is a compilation of work by a number of Shell geologists. In particular we would like to acknowledge the seismic interpretation of R. W. Allen, B. van Hoorn and A. van Vliet. Permission to publish was kindly granted by Shell Internationale Petroleum Maatschappij B.V., The Hague, Pecten Malaysia Co., Houston and PETRONAS, Kuala Lumpur.

REFERENCES

- ANDRESEN, A., and BJERRUM, L., (1976). Slides on subaqueous slopes in loose sand and silt. *In* Richards, A. F. (Ed.) *Marine Geotechnique*, pp 221–239, University of Illinois Press, Urbana.
- ARMGREN, A.A., (1978). Timing of Tertiary Submarine canyons and marine cycles of deposition in the Southern Sacramento Valley, California. *In* Stanley, D.J. and Kelling, G. (Ed.) *Sedimentation in submarine canyons, fans and trenches* Dowden, Hutchinson and Ross, Stroudsburg, Pennsylvania.
- BOL, A.J. and B. VAN HOORN, (1980). Structural styles in Western Sabah Offshore. *Bull. Geological Society of Malaysia* 12, pp 1–16.
- GARCIA, R., (1981). Depositional Systems and their Relation to Gas Accumulations in Sacramento Valley. *Am. Ass. Petr. Geol. Bull.* 65, 653–673.
- HAMILTON, W., (1979). Tectonics of the Indonesian Region. *U.S. Geological Survey. Prof. Pap.* 1078
- HANER, B.E. and GORSLINE, D.S., (1978). Processes and morphology of continental slope between Santa Monica and Dume Submarine Canyons, S. California. *Mar. Geol.* 28, 78–87.
- HOLLOWAY, N.H., (1981). The North Palawan Block Philippines: its relation to the Asian mainland and its role in the evolution of the South China Sea. *Bull. Geological Society Malaysia* 14, pp 19–58.
- JAUNICH, S., (1983). The Southwest African continental margin; buried palaeotopography. *In* Bally, A.W. (Ed). *Seismic Expression of structural styles*. Am. Ass. Pet. Geol. Studies in Geology 15 Vol. 1 1.2.6. AAPG, Tulsa, Oklahoma.
- VAIL P.R., R.M. MITCHUM and S. THOMPSON III., (1976). Seismic stratigraphy and global changes of sea level, Part 4: Global cycles of relative changes of sea level. *In* Payton, C.E. (Ed). *Seismic stratigraphy-applications to hydrocarbon exploration*. Am. Ass. Petrol. Geol. Mem. 26, 83–97. AAPG, Tulsa, Oklahoma.
- WESER, O.E., (1977). *Deep water oil sand reservoirs—ancient case histories and modern concepts*. Am. Ass. Pet. Geol. Course Note Ser. 6, AAPG, Tulsa, Oklahoma.

Manuscript received 17th May 1985.